

Retraction

Retracted: “Spectroscopic and Electrochemical Properties of $(1 - x)[\text{PVA/PVP}] : x [\text{MgCl}_2\{6\text{H}_2\text{O}\}]$ Blend Polymer Electrolyte Films”

International Journal of Polymer Science

Received 21 July 2019; Accepted 21 July 2019; Published 12 December 2019

Copyright © 2019 International Journal of Polymer Science. This is an open access article distributed under the Creative Commons Attribution License, which permits unrestricted use, distribution, and reproduction in any medium, provided the original work is properly cited.

International Journal of Polymer Science has retracted the article titled “Spectroscopic and Electrochemical Properties of $(1 - x)[\text{PVA/PVP}] : x [\text{MgCl}_2\{6\text{H}_2\text{O}\}]$ Blend Polymer Electrolyte Films” published in *International Journal of Polymer Science* in 2018 [1] due to figure duplication.

The journal initially received a request from the authors to correct Figures 1 and 2. During our assessment of the revised figures, it was identified that Figure 2 was a manipulated version of the original Figure. A further revised figure was also a duplicate of another previously published figure.

Following a reassessment of the published figures, the following issues were identified:

- (i) Figure duplication in Figure 1 in [1] with Figure 1 from [2]. In [1], the data is described as X-ray diffraction patterns of pure PVA/PVP blend polymer and with different wt% ratios of $\text{MgCl}_2 \cdot 6\text{H}_2\text{O}$, while in [2] the data is described as the X-ray diffraction pattern of PVA/PVP:GO
- (ii) Figure duplication in Figure 2B in [1] with Figure 2E from [3]. In [1], the data is described as the SEM images of $[\text{PVA/PVPMgCl}_2 \cdot 6\text{H}_2\text{O}] : x\%$ with different wt% compositions, while in [3] the data is described as SEM images of different compositions of $[\text{PVP} + \text{MgCl}_2 \cdot 6\text{H}_2\text{O}] : x\%$.
- (iii) Figure duplication in Figure 2D in [1] with Figure 3D from [4]. In [1], the data is described as the morphological surface of $[\text{PVA/PVPMgCl}_2 \cdot 6\text{H}_2\text{O}] : x\%$ with different wt% compositions, while in [4], the

SEM images are of pure PVP and $\text{PVP} + \text{MgSO}_4 \cdot 7\text{H}_2\text{O}$ with different wt% ratios

The authors responded to our concerns, however a satisfactory explanation was not provided.

We also asked the authors institutions to formally investigate. KL University responded to confirm the duplications but informed us that the accurate versions were published in [1], with the errors existing in the other publications; [2–4]. The corrections to these articles have since been published at [5–7], however, this article is being retracted due to concerns with the data. The authors do not agree to the retraction.

References

- [1] S. K. S. Basha and M. C. Rao, “Spectroscopic and Electrochemical Properties of $(1 - x)[\text{PVA/PVP}] : x [\text{MgCl}_2\{6\text{H}_2\text{O}\}]$ Blend Polymer Electrolyte Films,” *International Journal of Polymer Science*, vol. 2018, Article ID 2926167, 11 pages, 2018.
- [2] S. K. S. Basha and M. C. Rao, “Spectroscopic and discharge studies on graphene oxide doped PVA/PVP blend nanocomposite polymer films,” *Polymer Science, Series A*, vol. 60, no. 3, pp. 359–372, 2018.
- [3] S. K. S. Basha and M. C. Rao, “Spectroscopic and electrochemical properties of PVP based polymer electrolyte films,” *Polymer Bulletin*, vol. 75, no. 8, pp. 3641–3666, 2018.
- [4] S. K. S. Basha, G. S. Sundari, K. V. Kumar, and M. C. Rao, “Preparation and dielectric properties of PVP-based polymer electrolyte films for solid-state battery application,” *Polymer Bulletin*, vol. 75, no. 3, pp. 925–945, 2018.

- [5] S. K. S. Basha and M. C. Rao, "Correction to: Spectroscopic and electrochemical properties of PVP based polymer electrolyte films," *Polymer Bulletin*, pp. 1-2, 2019.
- [6] S. K. S. Basha, G. S. Sundari, K. V. Kumar, and M. C. Rao, "Correction to: Preparation and dielectric properties of PVP-based polymer electrolyte films for solid-state battery application," *Polymer Bulletin*, p. 1, 2019.
- [7] S. K. S. Basha and M. C. Rao, "Erratum to: Spectroscopic and Discharge Studies on Graphene Oxide Doped PVA/PVP Blend Nanocomposite Polymer Films," *Polymer Science, Series A*, vol. 61, no. 2, pp. 226–229, 2019.

Research Article

Spectroscopic and Electrochemical Properties of $(1 - x)[\text{PVA/PVP}] : x[\text{MgCl}_2 \cdot 6\text{H}_2\text{O}]$ Blend Polymer Electrolyte Films

Sk. Shahenoor Basha¹ and M. C. Rao ²

¹Solid State Ionics Laboratory, Department of Physics, KL University, Guntur 522502, India

²Department of Physics, Andhra Loyola College, Vijayawada 520008, India

Correspondence should be addressed to M. C. Rao; raomc72@gmail.com

Received 29 September 2017; Revised 13 November 2017; Accepted 14 December 2017; Published 18 January 2018

Academic Editor: Cornelia Vasile

Copyright © 2018 Sk. Shahenoor Basha and M. C. Rao. This is an open access article distributed under the Creative Commons Attribution License, which permits unrestricted use, distribution, and reproduction in any medium, provided the original work is properly cited.

Blend polymer electrolytes were prepared with different wt% compositions of $[\text{PVA/PVP-MgCl}_2 \cdot 6\text{H}_2\text{O}] : x\%$ using solution cast technique. Structural, morphological, vibrational, thermal, and ionic conductivity and electrochemical properties were studied on the prepared polymer films. XRD revealed the crystalline nature of the polymer electrolyte films. The morphology and the degree of roughness of the prepared films were analyzed by SEM. FTIR and Raman studies confirmed the chemical complex nature of the ligands, interlinking bond formation between the blend polymers and the dopant salt. The glass transition temperature (T_g) of polymer electrolytes was confirmed by DSC studies. Ionic conductivity measurements were carried out on the prepared films in the frequency ranging between 5000 Hz and 50000 KHz and found to be maximum (2.42×10^{-4} S/cm) for the prepared film with wt% composition 35PVA/35PVP : 30MgCl₂·6H₂O at room temperature. The electrochemical studies were also performed on the prepared films. The galvanostatic charge/discharge performance was carried out from 2.9 to 4.4 V for the configuration $\text{Mg}^+ / (\text{PVA/PVP} + \text{MgCl}_2 \cdot 6\text{H}_2\text{O}) / (\text{I}_2 + \text{C} + \text{electrolyte})$.

1. Introduction

Over the past few decades, batteries are a primary source for high energy density. They play an important role in energy storage device applications [1, 2]. Blend polymer electrolytes with complex nature of organic or inorganic salts have been analyzed to prepare energy devices, as they have potential and electrochemical properties [3]. These can be used in many industrial and energy storage device applications such as solid state batteries, fuel cells, and electrochromic display devices/smart windows [4, 5]. One of the main objectives is to develop the blend polymer systems with enhanced ionic conductivity. There are several strategies in solid polymer electrolyte (SPE) systems to suppress the crystalline nature. Polymers can be classified in to subgroups like block copolymers [6, 7], polymer blends [8, 9], cross-linked polymer networks [10, 11], and comb-branched copolymers [12–15]. Blend

polymer electrolytes were used in the fabrication of electrochemical cells and thin film solid state batteries. Due to low negligible hazards magnesium rechargeable batteries are used now a days in many applications such as microbatteries and energy storage devices. They can be operated safely at room temperature [16, 17].

Blending of polymers is one of the promising methods which are used in wide variety of applications such as energy storage devices, electrochemical cells, fuel cells, and humidity sensors, to attain high ionic conductivity. In recent years, research on blending of polymers has given a fascinating change in the pharmaceutical and industrial practice due to their desired properties. Blending of polymers with suitable organic and inorganic salt can give better improvement in ionic conductivity which can lead to the same order of ionic conductivity for the salt doped single polymer. However, their ionic conductivity is usually limited by segmental mobility

and concentration of charged carriers. Some of the plasticizers such as propylene carbonate (PC) and ethylene carbonate (EC) and inorganic nanofillers have been incorporated into the polymer blend electrolytes to increase the flexibility or plasticity of the polymers as well as to enhance the ionic conductivity to be comparable to the lithium electrolytes. Ion transport mechanism in the polymer electrolytes is one of the key notes to understand how the enhancement of ionic conductivity through host polymer matrix takes place. Different methods have been used to increase the ionic conductivity, such as cross-linking of two polymers, adding of plasticizers to polymer electrolytes, adding inorganic inert fillers, and blending two polymers. Certain problems arise when fabricating polymer films with improved ionic conductivity like high cost, ease of film formation, and less durability of battery. To overcome these problems polymer blends have been prepared. In general polymer blends should be completely soluble in the proper solvent but differ in chemical structure which cause miscibility problems at a molecular level. However, the film properties depend upon the miscibility of the components of the blend.

The complex nature of polymer blends is physically similar but structurally different and has interlinking with hydrogen bonding, ionic and dipole interactions. By mixing two polymers the ionic conductivity can be easily increased. Moreover the physical and mechanical properties of the film depend upon the miscibility of the polymer blend such as charge transfer complexes for homopolymer mixtures [18]. In the present investigation blend polymers like polyvinyl alcohol (PVA) and polyvinyl pyrrolidone (PVP) were chosen because of their excellent physical, mechanical, and electrochemical properties. Of all the polymers PVA is the most extensively studied one as it has multiple potential applications. It is used as an electrode material in secondary batteries and microelectronics and also as an electrochromic display material [19, 20]. PVP polymer is made up of several branches of monomers and it is also known as N-vinylpyrrolidone. PVP is easily soluble in ionized water, has excellent wetting properties, and readily forms films [21, 22]. Polyvinyl alcohol is an exceptional polymer having high electrical, optical, and mechanical properties. PVA has high tensile strength, good charge storage capacity, and excellent film forming nature. PVA and PVP polymers are ecofriendly and biodegradable polymers. Because of their polar groups, they are easily soluble in water as well as in organic suitable solvents. The purpose of this work is to attain high ionic conductivity and stabilized electrochemical properties from the blend polymer electrolytes by the dissolution of inorganic salt in the host lattice. The prime novelty of this investigation is to develop and characterize the prepared blend polymer electrolytes with improved physical and electrical properties at laboratory scale. Cost effective solution cast technique is used for the preparation of polymer electrolytes in order to develop conventional alternative sources of energy [23].

Magnesium metal (Mg^{2+}) is a very important element, easily available in the earth crust, and much cheaper than lithium (Li^+). Magnesium metal can be used as an anode material for solid state batteries. The ionic radii and magnitude of magnesium metal are less when compared to

lithium. Moreover magnesium metal is more stable, less toxic, nonexplosive, and can be handled safely in oxygen and humid atmosphere. Magnesium chloride hexahydrate is easily soluble in water and it can be used as a binary agent in pharmaceuticals, industrial, agriculture purposes, and so on. From the literature survey it was confirmed that the study on blend polymer with the complexation of inorganic salts for the fabrication of electrochemical cells is scarce. The main objective of the present investigation is to prepare a solid polymer electrolyte film using PVA/PVP polymer blend with different wt% ratios of $MgCl_2 \cdot 6H_2O$, that is (45/45 : 10, 40/40 : 20, 35/35 : 30). The prepared films were characterized by X-ray diffraction (XRD), scanning electron microscopy (SEM), Fourier transform infrared spectroscopy (FTIR), differential scanning calorimetry (DSC), Raman spectroscopy, AC impedance spectroscopy, and cyclic voltammetry (CV) studies.

2. Experimental

2.1. Sample Preparation. The chemicals used in the present investigation are magnesium chloride hexahydrate (99.5% purity) with molecular weight 203.30 and nitrate (NO_3^-): $\leq 0.001\%$; polyvinyl alcohol (PVA): average molecular weight = 89,000–98,000 and molecular weight of repeat unit: 44.00 g/mol; and polyvinyl pyrrolidone (PVP): average molecular weight = 36,000–40,000 and molar mass of PVP is 112.88902 ± 0.00010 g/mol. All chemicals used in the present investigation were purchased by us from Sigma Aldrich chemicals Ltd., India. Blend polymer electrolyte films were prepared in different wt% ratios (90 : 10, 80 : 20, and 70 : 30) by doping magnesium chloride hexahydrate in the host polymer by solution cast technique. Stir all the mixtures till the polymers get dissolved in water for 48 hrs. Finally the obtained composite solution was poured in polypropylene dishes and placed in hot air oven at $70^\circ C$. A fine nanocomposite polymer thin film was obtained. The prepared film was kept in a desiccator until further test.

2.2. Characterization. X-ray diffraction (XRD) studies were performed by using a Philips analytical X'pert diffractometer in the diffraction " 2θ " angular range $10-70^\circ$ with nickel filtered $CuK\alpha$ radiation ($\lambda = 1.5403 \text{ \AA}$). Fourier transform infrared (FTIR) spectra were recorded with the help of a Perkin Elmer Alpha-E Spectrophotometer and heater coil of the furnace recorded in the wavenumber range $650-4000 \text{ cm}^{-1}$. The thermal analysis and heat flow in a sample were measured by differential scanning calorimeter (DSC), Q-2920, TA and which gives the information about the quantitative and qualitative analysis. Morphological studies were carried out on the prepared samples with different resolutions by using FE-SEM, Carl Zeiss, Ultra 55 model. The complex formation between the polymer and the salt was characterized by a Nano finder 30 SOLAR TII laser Raman spectroscope. The impedance measurements of the prepared films were carried out in the frequency ranging between 5000 Hz and 50000 KHz on HIOKI 3532-50 LCR Heister. Solid state battery has been fabricated with the configuration Mg^+ (anode)/polymer electrolyte/(I

TABLE 1: FWHM, AC conductivity, and transport values of polymer electrolyte films for different wt% ratios.

Blend polymer films	FWHM values (nm)	AC conductivity values of (PVA/PVP + MgCl ₂ ·6H ₂ O) polymer electrolyte system	Transport properties of PVA/PVP : MgCl ₂ ·6H ₂ O blend polymer electrolyte films	
		Conductivity at room temperature (S/cm)	t_{ion}	t_{ele}
PVA/PVP: (50 : 50)	6.19251	4.32×10^{-6}	—	—
PVA/PVP : MgCl ₂ ·6H ₂ O (45/45 : 10)	9.2407	6.12×10^{-5}	0.96	0.04
PVA/PVP : MgCl ₂ ·6H ₂ O (40/40 : 20)	11.85137	3.52×10^{-5}	0.97	0.03
PVA/PVP : MgCl ₂ ·6H ₂ O (35/35 : 30)	13.89526	2.42×10^{-4}	0.99	0.01

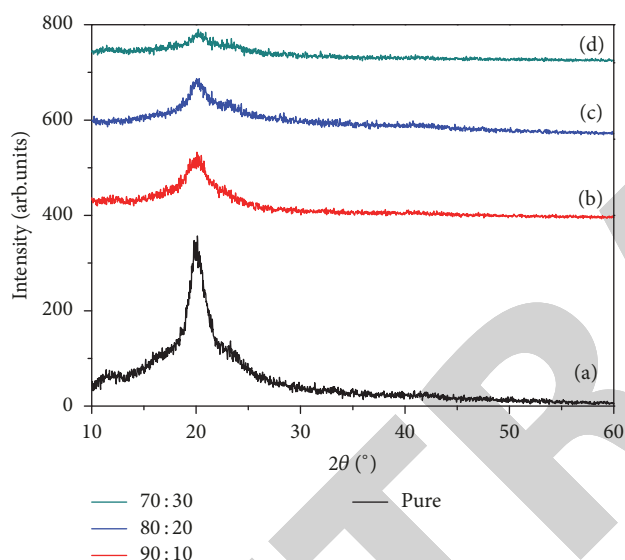


FIGURE 1: XRD pattern for different wt% ratios of composite polymer electrolyte films.

+ C + electrolyte)/(cathode) for a constant load of 100 kΩ at room temperature by Keithley electrometer 5641. The charge/discharge performance was carried out from 2.9 to 4.4 V.

3. Results and Discussion

3.1. XRD Analysis. X-ray diffraction patterns of pure PVA/PVP blend polymer and with different wt% ratios of MgCl₂·6H₂O salt, that is, (90 : 10), (80 : 20), and (70 : 30), were shown in Figure 1. XRD pattern showed a broad peak at 20° ascribed to the pure PVA/PVP which corresponds to orthorhombic lattice indicating its semicrystalline nature. From Figure 1, it was observed that the intensity of the peak is gradually decreased with the increase in salt concentration. It confirms that the salt is completely dissolute in the host polymer for higher concentration 30 wt% ratio; no sharp peaks were observed due to the dissolution of salt within the polymer which turns the semicrystalline to amorphous

phase [24, 25]. The intensity of the PVA/PVP diffraction peak decreases with the increase in the wt% ratio of MgCl₂·6H₂O salt. This may be due to the increase of the softness of the polymer chains where the molecular chains are irregular and entangled in amorphous regions rather than crystalline region. From XRD spectra it is clearly observed that the peak intensity is gradually decreased. As a result full width half maxima (FWHM) of the peak has widened due to flexible backbone and crystalline nature of the polymer. The decrease of degree of crystalline nature was formed due to the dissolution of salt in the polymer matrix. The FWHM values of the peaks were presented in Table 1.

3.2. SEM Studies. The morphological surface of [PVA/PVP-MgCl₂·6H₂O]:x% with different wt% compositions was shown in Figure 2. Figure 2 showed the phase formation of blend polymer electrolyte system. It was also observed that inorganic salt chunks with different degrees of roughness at different resolutions were found in Figures 2(a), 2(b), and 2(c). The presence of salt chunks possesses crystalline phase in rest of the samples which was clearly shown in XRD pattern [26]. The crystalline peaks having less intensity were attributed to salt particles in the polymer chains. But from Figure 2(d), no phase separation was observed for (35/35 : 30) electrolyte system. This may be due to the dissolution of MgCl₂·6H₂O salt in the host PVA/PVP polymer.

It was also observed from the Figure 2 that small chunks were formed due to the dispersion of MgCl₂·6H₂O : x% for 10, 20, and 30 wt% ratios in the PVA/PVP polymer matrix. It results in the dopant salt being incompletely soluble in the host polymer. It is noticed that for 30 wt% ratio dispersion takes place and no phase separation has been observed in the host polymer which enhances the ionic conductivity. As the wt% of MgCl₂·6H₂O increase, the degree of roughness of the films is decreased. This shows the amorphous nature of the film. The higher level of MgCl₂·6H₂O in PVP/PVA will result in better dispersion in blend polymer matrix resulting in the enhancement of ionic conductivity, which is confirmed from SEM images. This agrees with XRD analysis.

3.3. FTIR Studies. FTIR is a versatile instrument to identify the chemical complex nature among the polymer matrix and

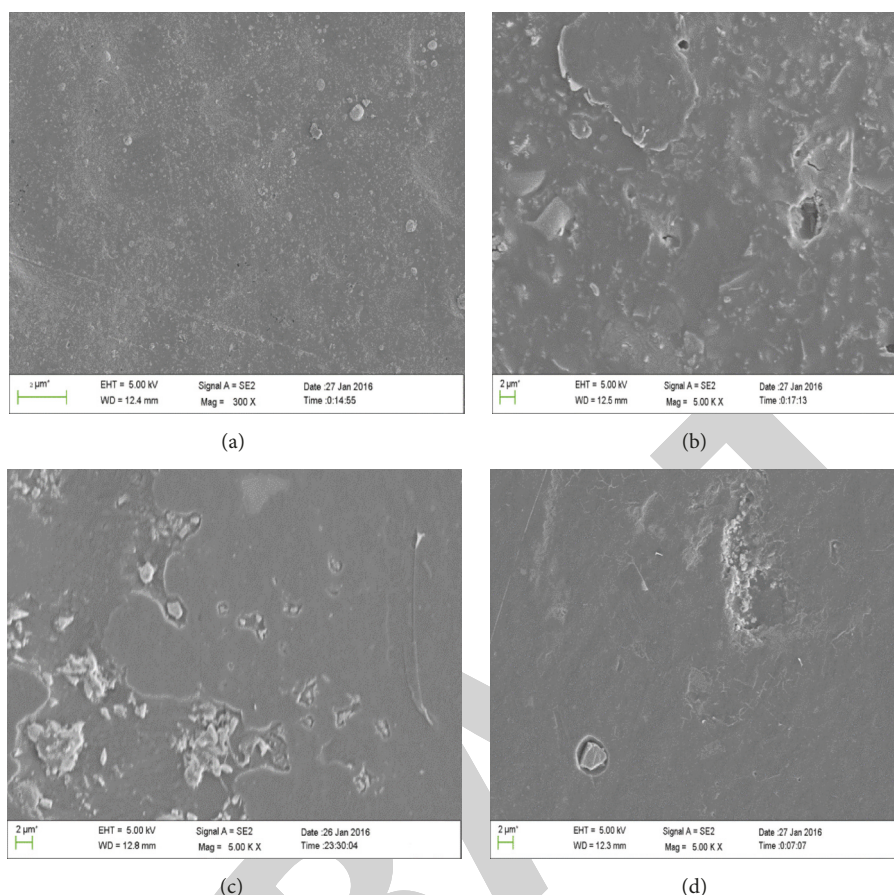


FIGURE 2: SEM images for different wt% ratios of composite polymer electrolyte films.

encapsulation of different elements in functional groups [27]. The thickness of the prepared films was calculated by wedge method and it was found to be $110\ \mu\text{m}$. In the present investigation FTIR spectra of blend polymer of pure PVA/PVP and mixed with different wt% ratios of $\text{MgCl}_2 \cdot 6\text{H}_2\text{O}$ in the wavenumber ranging between 650 and $4000\ \text{cm}^{-1}$ is shown in Figure 3. An interaction takes place by doping the salt into the polymer matrix and the complex nature occurs between the salt and the host polymer matrix. The vibrational bands observed at 1000 , 1500 , 1570 , and $1820\ \text{cm}^{-1}$ corresponded to C–H bending and C–H₂ stretching of hydroxyl group and C=O carboxyl group, respectively [28]. With the increase in the wt% ratio, the stretching, bending intensity of the peaks appeared in the wavenumber region 1150 – $1750\ \text{cm}^{-1}$ and the band corresponding to the wavenumber region 2900 – $3800\ \text{cm}^{-1}$ indicates the outer phase vibration oscillation of the hydroxyl group O=H which is completely mixed with the polymer further. From the figure it has been observed that the width of the vibrational bands of pure PVA/PVP at 1350 , 1470 and $1650\ \text{cm}^{-1}$ changes with the increase of dopant concentration. There is a difference in the spectral range that has been observed on comparing with the pure PVA/PVP. This is due to the stretching and bending of the ions which are completely mixed with the host polymer [29]. In addition C–H bending vibrations take place in the

region 1000 – $3800\ \text{cm}^{-1}$ while the band at $1670\ \text{cm}^{-1}$ indicates that the cations of the salt get coordinated with the oxygen of PVA/PVP blend polymer. This is due to the change in the width of the spectral peaks. The shifts in the band positions may be attributed to the complex formation between PVA/PVP and $\text{MgCl}_2 \cdot 6\text{H}_2\text{O}$ salt. This influences the local structure of polymer backbones and significantly affects its mobility [30].

3.4. DSC Analysis. Differential scanning calorimetry is an effective tool for analyzing the thermal analysis of the materials such as glass transition temperature (T_g) and melting temperature (T_m) in the polymer electrolytes. The DSC spectra of PVA/PVP : $\text{MgCl}_2 \cdot 6\text{H}_2\text{O}$ polymer films with different wt% ratios were shown in Figure 4. It is observed from the figure that, with increase of wt% ratio of salt in the host polymer, the glass transition temperature (T_g) of polymer electrolytes decreased and was found to be at 98 , 92 , 84 , and 81°C . From the DSC curves, it is observed that solid polymer films exhibited only single T_g value due to the miscibility of the salt in the polymer matrix. The decrease in T_g takes place due to lubricating effect of the polymer chains for $35/35 : 30$ wt% ratio of the sample at 81°C . This lubrication effect occurs due to the formation of free spaces around polymer chains. The lowering of T_g is expected to make the

TABLE 2: Raman bands and wavenumber assignments of polymer electrolyte films for different wt% ratios.

PVA/PVP : MgCl ₂ ·6H ₂ O (45/45 : 10)	Wavenumber (cm ⁻¹) PVA/PVP : MgCl ₂ ·6H ₂ O (40/40 : 20)	PVA/PVP : MgCl ₂ ·6H ₂ O (35/35 : 30)	Assignment
810	790	785	C–C stretching
1410	1410	1402	C–N stretching
1710	1780	1795	O–H bending
—	1820	1860	C–O rocking

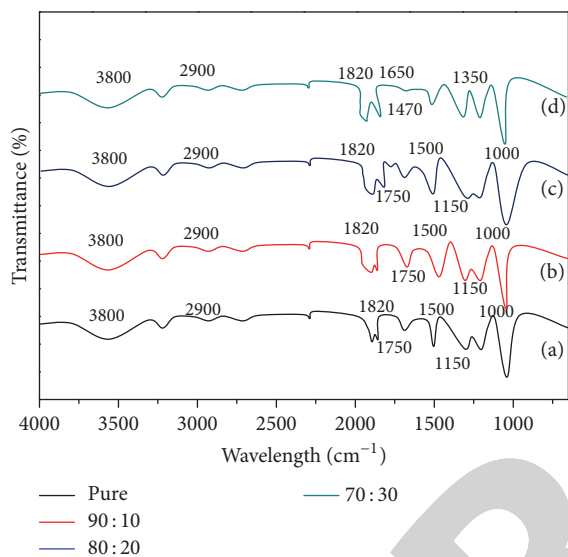


FIGURE 3: FTIR spectra for different wt% ratios of composite polymer electrolyte films.

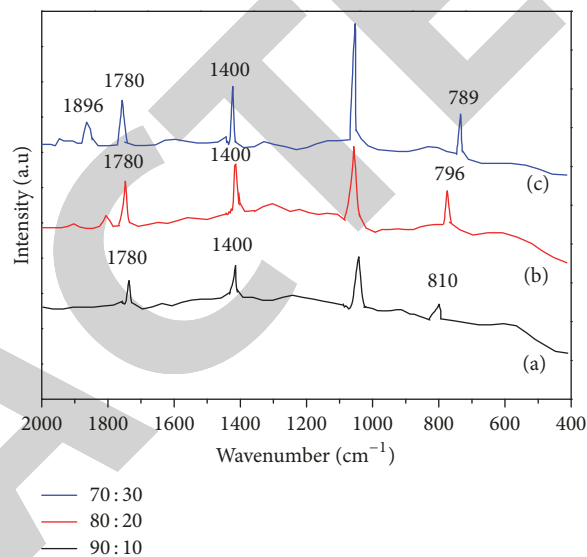


FIGURE 5: Raman spectra for different wt% ratios of composite polymer electrolyte films.

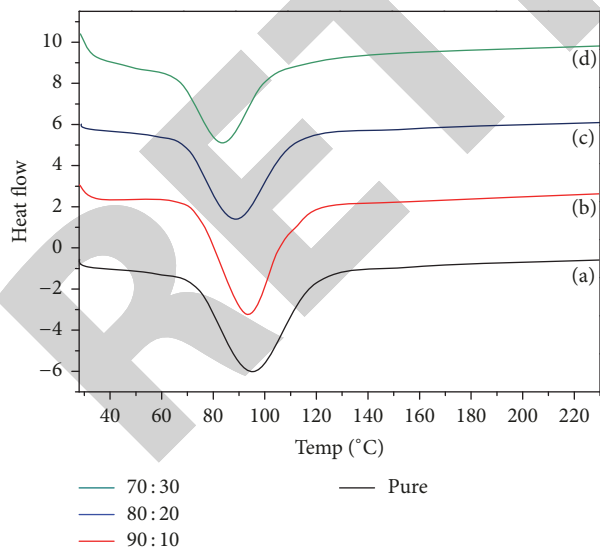


FIGURE 4: DSC spectra for different wt% ratios of composite polymer electrolyte films.

ions move easily in the prepared polymer electrolyte system [31]. Similar results were reported by Varnell and Coleman for PVA : CH₃COONH₄ polymer electrolyte system [32]. In addition, the melting temperature of endothermic peak is

shifted towards the lower temperature with increase of salt concentration. It reveals the decrease of crystalline nature and dominant presence of amorphous phase [33].

3.5. Raman Studies. Figure 5 represents the Raman spectra of PVA/PVP blend polymer with different wt% ratios of MgCl₂·6H₂O (10%, 20% and 30%) in the wavenumber region 400–2000 cm⁻¹ at room temperature and their vibrational band assignments were presented in Table 2. From Figure 5, it was observed that the Raman bands at 810, 1410, and 1780 cm⁻¹ correspond to C–C stretching, C–N stretching, C–O rocking, O–H bending, and C–H bending vibration for mixed polymer films, respectively [34, 35]. The peak intensity of Raman bands has been changed due to the addition of different wt% ratios of MgCl₂·6H₂O in the blend polymer matrix. The intensity of the Raman band at 1400 cm⁻¹ corresponds to C–C stretching and is decreased with the increase of wt% ratio of salt concentration in the polymer [36]. A new additional peak with less intensity has been observed in the above spectrum at 1780 cm⁻¹ and it is due to the presence of Mg²⁺ ion in the polymer [37]. The introduction of these new peaks in the salt doped system is due to the interaction of proton with carbonyl and hydroxyl groups. The significant changes in the above

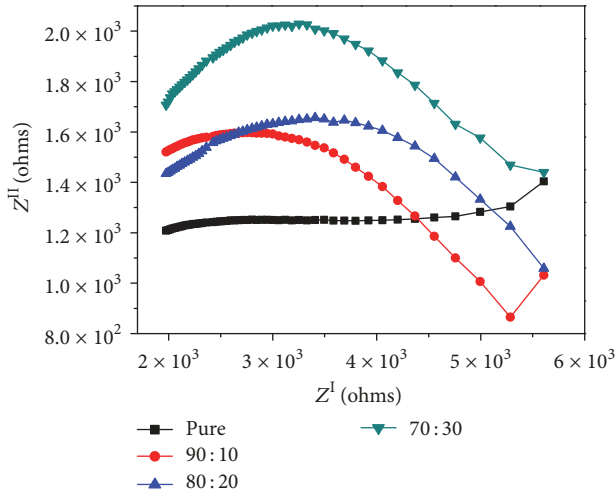


FIGURE 6: Cole-Cole plots for different wt% ratios of composite polymer electrolyte films.

bands can be related to the interaction of the salt with the polymer.

3.6. AC Conductivity Studies. Cole-Cole plot gives the information about the ionic conductivity of the prepared materials. In general Cole-Cole plot shows a semicircle region at high frequency region which is due to parallel combination of resistor and capacitor and a spike is obtained at low frequency due to the migration of ions at the electrode–electrolyte interface. Complex independence spectroscopy for the prepared samples for different wt% ratios is shown in Figure 6. But from the figure it is observed that only spikes were obtained for all the wt% compositional ratios. It may be due to the majority charge carrier flow of ions, where the electronic polarization occurs in the solid polymer electrolyte at electrode–electrolyte interface [38]. The impedance plot can be analyzed by varying real part (Z^I) with respect to the imaginary part (Z^{II}) and the ionic conductivity is calculated by the following relation:

$$\sigma_{ac} = \frac{t}{(R_b \times A)}, \quad (1)$$

where “ R_b ” is the bulk resistance, “ t ” is the thickness of the solid polymer electrolyte, and “ A ” is the area of the electrolyte. The calculated AC conductivity values are presented in Table 1.

3.7. Transport Properties. The transport (transference) number (t) of the sample indicates the sum of total ionic and electronic current in terms of the total conductivity (σ). The ionic transference number is defined as the ratio of transference number of any particles/ions to total conductivity (σ_T) [39]. The electronic transference number is defined as the ratio of transference number of electronic/hole conductivity to total conductivity (σ_T). The transport properties have been calculated by the following equations

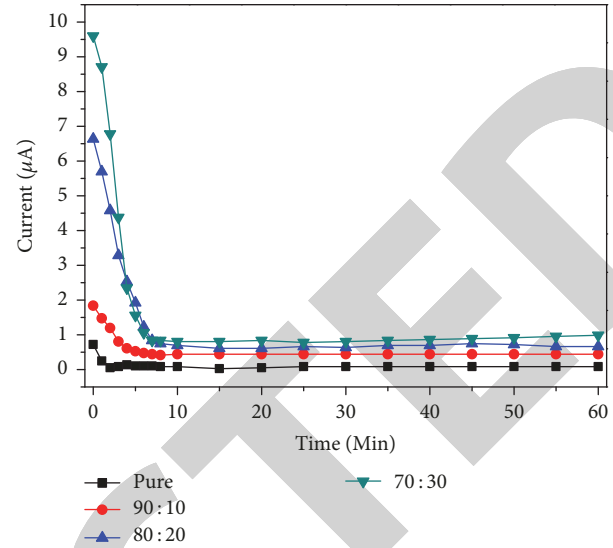


FIGURE 7: Transport properties for different wt% ratios of composite polymer electrolyte films.

using Wagner’s polarizing technique which is presented in Table 1.

$$t_{ion} = i_t - \frac{i_{ele}}{i_t}, \quad (2)$$

$$t_{ele} = \frac{i_{ele}}{i_t},$$

where i_t is the initial current and i_{ele} is the final residual current for all compositions of PVA/PVP : $MgCl_2 \cdot 6H_2O$ electrolyte systems. The current versus time plots were shown in Figure 7. Initially, the current (i_t) increases then immediately decays and reaches a steady state after a long time of polarization takes place. This may be due to the current initially flowing across the cell at the blocking electrode under the influence of an applied voltage. Initially, after the application of DC potential the total current across the cell is proportional to the applied field due to the migration of ions or electrons (i_t or $i_t = i_{ion} + i_{ele}$). At the blocking electrode, there is neither a source nor a sink for mobile ions. The migration of the ions under the influence of the electric field therefore leads to an enrichment of the mobile species in the electrolyte region. Thus the current starts decreasing with time as the drift of ions is balanced by diffusion of ions due to their concentration gradient induced by the electrode which blocked the ions, but still active towards electrons and hence the cell gets polarized. Thus it is apparent that during DC polarization, the interfacial resistance increases due to the formation of passivation layer of ions at the interface of blocking electrode. As a result the ionic current is blocked, the polarization is exclusively carried by electrons, and hence the final current is only due to electronic current ($i_f = i_{ele}$). The values of ionic transference number are in the range 0.96–0.99. These results state that the charge carriers are mainly due to ions and negligible contribution takes place from electrons [40].

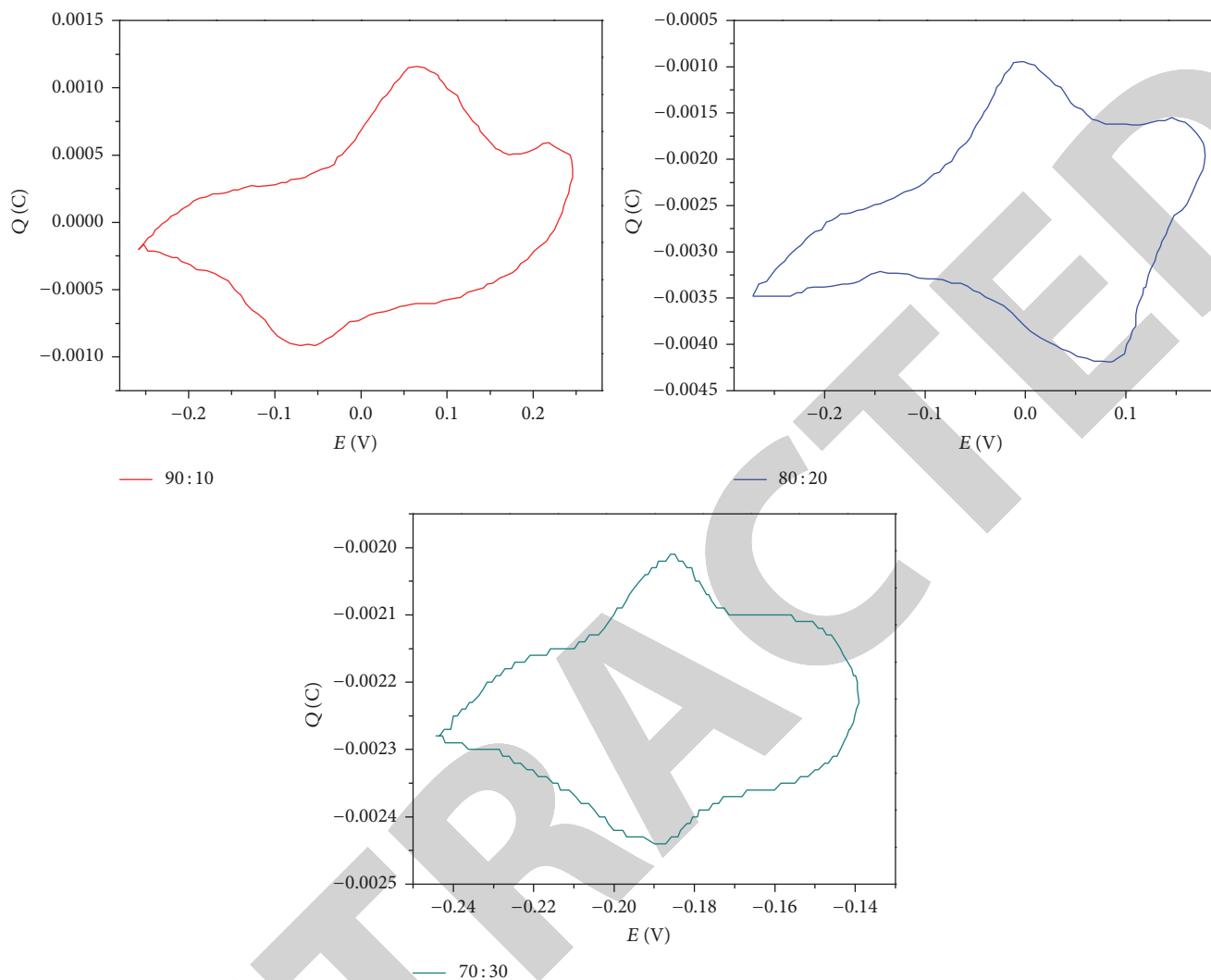


FIGURE 8: Cyclic voltammetry for different wt% ratios of composite polymer electrolyte films.

3.8. Cyclic Voltammetry. Cyclic voltammetry has been carried out between the sweep potential and charge to evaluate the chemical and electrochemical stability of the solid polymer electrolytes. The electrochemical studies of the polymer electrolytes based on ILs (Figure 8) were determined by microelectrode cyclic voltammetry over the potential ranging from -2.0 to 6.0 V at scan rate $30 \text{ mV}\cdot\text{s}^{-1}$ in ambient temperature. The peak currents decrease with the increase of the scan numbers. This may be due to the detachment of the samples from the electrode surface [41, 42]. Cyclic Voltammetry curves have been measured for different wt% ratios of mixed blend polymer electrolytes which are shown in Figure 8. The CV curve showed the oxidation peak at 0.5 V and reduction peak at 0.2 V. The oxidation peak is attributed to the conversion of magnesium chloride into magnesium. The reduction of iodine and carbon is soluble in magnesium. The area of oxidation and reduction peaks decreased continuously with repeated cycling [43]. The reduction peak at 2.9 V disappeared after 7 hours, which is shown in Figure 9.

3.9. Polarization Studies. Electrochemical cell has been fabricated for the maximum ionic conductivity obtained polymer electrolyte film (35PVA/35PVP : $30\text{MgCl}_2\cdot 6\text{H}_2\text{O}$). The electrochemical studies were performed on the prepared films. The galvanostatic charge/discharge performance was carried out from 2.9 to 4.4 V for the configuration $\text{Mg}^+ / (\text{PVA}/\text{PVP} + \text{MgCl}_2\cdot 6\text{H}_2\text{O}) / (\text{I}_2 + \text{C} + \text{electrolyte})$. The electrode materials were made in the form of a pellet with the thickness of 1 mm. The electrochemical stability is found to be stable up to ~ 4.5 V for 35PVA/35PVP : $30\text{MgCl}_2\cdot 6\text{H}_2\text{O}$ electrolyte film. In the fabrication of electrochemical cell, magnesium metal is used as anode material where the charge carriers take place at the electrolyte region and the combination of iodine, carbon powder, and electrolyte film traces are used as cathode for enhancement of electronic conductivity [44]. The discharge capacity of an electrochemical cell is shown in Figure 10. From the figure it is observed that the discharge capacity is decreased during sixth cycle and gradually declined with subsequent cycling. This may be due to the magnesium ions which are attributed at the electrode–electrolyte interfaces,

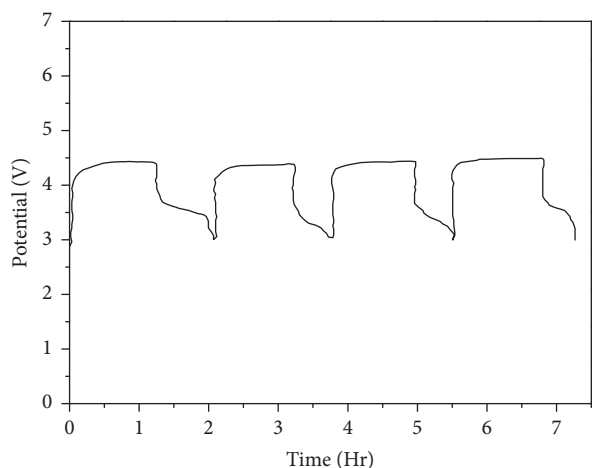


FIGURE 9: Variation of time versus potential of composite polymer electrolyte films for (70 : 30) wt% ratio.

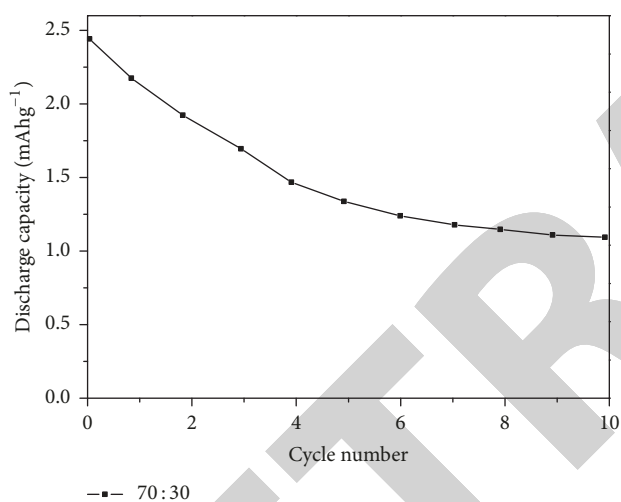


FIGURE 10: Variation of cycle number with discharge capacity of solid polymer electrolyte films for (70 : 30) wt% ratio.

whereas the surface of the film changes during the repeated cycling. Surface films block the charge transfer reaction between Mg anode and solid polymer electrolyte, since the mobility of Mg^{2+} ions in the passivation of films becomes extremely small [45].

Charge-discharge profiles of the prepared cell are shown in Figure 11(a). The current density has been measured for the prepared solid polymer battery at $30 \mu A cm^{-1}$ between 4.0 and 0.6 V. During the cyclic process, the potassium ions get diffused 10 to 30% in the polymer matrix which is measured at $8.5 Ah cm^{-2}$. The discharge voltage gradually decreases from 2.65 to 0.6 V, probably because of the amorphous nature of the PVA/PVP film. This initial capacity loss is explained by inserted K^+ ions to produce the metallic alloy and amorphous region, which causes an irreversible capacity. However, after the first discharge, there is a continuous decrease in the charge and discharge capacity. This cell can be cycled for more than 200 cycles maintaining good efficiency. The cell

can discharge at a current density up to $250 \mu A cm^{-2}$ for the potential drop across the resistance cell. Initially, the voltage across the cell has been raised from 2.9 V and stabilized to 4.1 V. The performance of the cell capacity has been raised up to 1.6 Hrs and becomes constant after certain time till 3.5 Hrs. This may be due to the polarization taking place across the electrode and electrolyte interface. When an amount of voltage is applied across the cell, the K^+ ions diffuses and transfers from anode to the cathode layer through the electrolyte medium and the complete cycling course was done at the room temperature which is shown in Figure 11(b). The capacity retention has been measured with respect to the cycle number in the ambient temperature shown in Figure 11(c). The capacity retention of 50% is achieved at $-5^{\circ}C$ at moderate discharge rate of 0.5 C. The GSM pulse discharge mode (1.5 A for 6 ms/0.15 A for 4 ms) was applied to cell at various temperatures and capacity retention was determined.

3.10. Electrochemical Properties. The fabricated cell was allowed to equilibrate for 30 min and the OCV was measured which is at 2.9 V. The cell was cycled galvanostatically at $10 \mu A$ and the electrochemical performance is shown in Figure 12. As depicted, the charging curve (plateau potential) indicates that Mg^{2+} deintercalation occurs at the cathode. Figure 12 depicts the open circuit voltage of the $Mg^{+}/(PVA/PVP + MgCl_2 \cdot 6H_2O)/(I_2 + C + electrolyte)$ cell. Various cell parameters such as open circuit voltage (OCV), power density, and current density have been evaluated and shown in Figure 13. Initially a rapid decrease in the voltage occurred. It may be due to the polarization and the formation of thin layer of magnesium salt at the electrode/electrolyte interfaces [46]. It was observed that the fabricated cell showed the OCV at 2.9 V for about 24 h when the test was terminated. The mixed polymer electrolyte for the composition 35PVA/35PVP : 30MgCl₂·6H₂O exhibited better performance than the other wt% ratios, which strongly suggests that wt% of 35PVA/35PVP : 30MgCl₂·6H₂O polymer blend electrolyte film is more suitable in the fabrication of solid state polymer batteries.

4. Conclusions

Blend polymer electrolytes were prepared with different wt% compositions of [PVA/PVP-MgCl₂·6H₂O] : x% using solution cast technique. The crystalline phase of the blend polymer electrolytes was confirmed by XRD analysis. FTIR and Raman studies confirmed the chemical complex nature and interlinking bond formation between the blend polymers and dopant salt. SEM revealed the degree of roughness of the prepared films at different resolutions. The glass transition temperature of the polymer electrolytes was decreased with increasing wt% ratio of the host polymer. The maximum ionic conductivity of $2.42 \times 10^{-4} Scm^{-1}$ was found for the composition 35PVA/35PVP : 30MgCl₂·6H₂O of the polymer blend electrolyte. The transference number of the prepared films was calculated by Wagner's polarization technique. The electrochemical cell was fabricated and the cell parameters

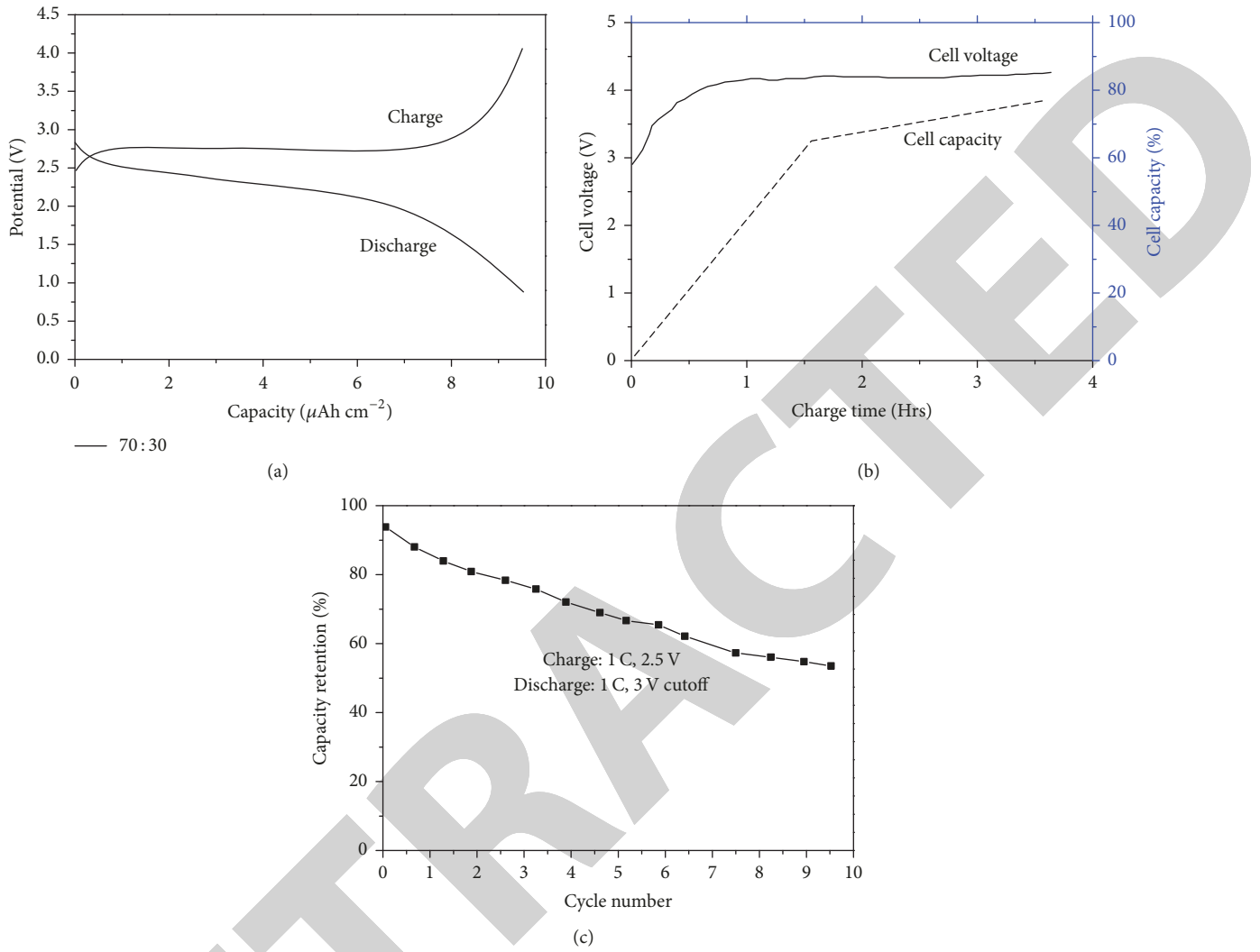


FIGURE 11: (a) Potential versus capacity curves of solid polymer electrolyte film for (70 : 30) wt% ratio. (b) Cell voltage versus charge time versus cell capacity of solid polymer electrolyte film for (70 : 30) wt% ratio. (c) Capacity retention versus cycle number of solid polymer electrolyte film for (70 : 30) wt% ratio.

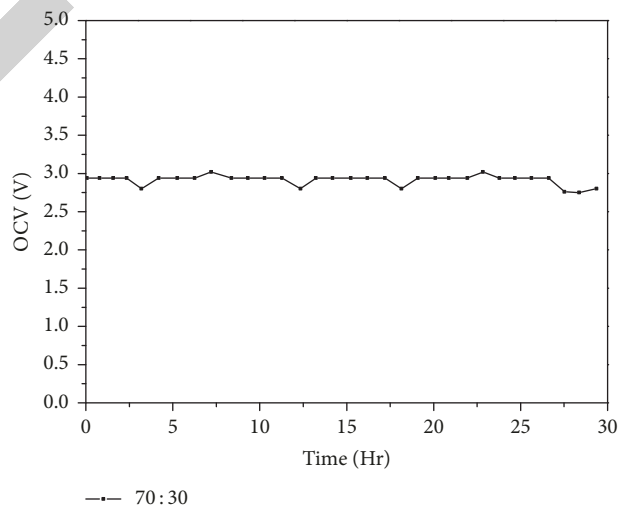


FIGURE 12: OCV of solid polymer electrolyte film for (70 : 30) wt% ratio.

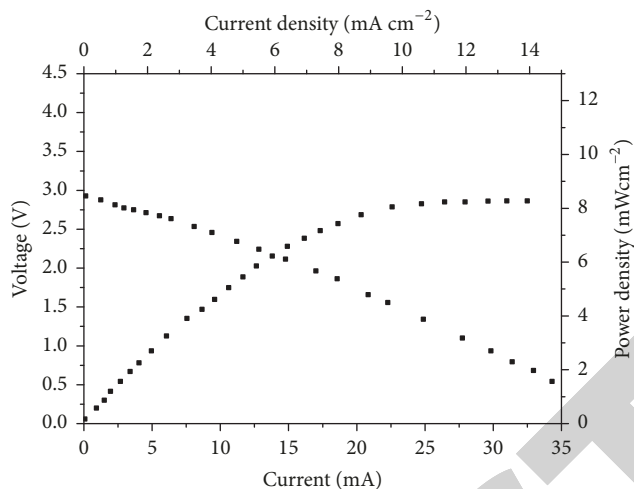


FIGURE 13: Cell parameters of solid polymer electrolyte film for (70 : 30) wt% ratio.

were evaluated for 35PVA/35PVP : 30MgCl₂·6H₂O polymer electrolyte film.

Conflicts of Interest

The authors declare that there are no conflicts of interest regarding the publication of this paper.

References

- [1] C. Manea and M. Mulder, "New polymeric electrolyte membranes based on proton donor-proton acceptor properties for direct methanol fuel cells," *Desalination*, vol. 147, no. 1-3, pp. 179–182, 2002.
- [2] P. Corbo, F. Migliardini, and O. Veneri, "Dynamic behaviour of hydrogen fuel cells for automotive application," *Journal of Renewable Energy*, vol. 34, no. 8, pp. 1955–1961, 2009.
- [3] M. Morita, J.-L. Qiao, N. Yoshimoto, and M. Ishikawa, "Application of proton conducting polymeric electrolytes to electrochemical capacitors," *Electrochimica Acta*, vol. 50, no. 2-3, pp. 837–841, 2004.
- [4] N. G. Bukun, E. I. Moskvina, and E. A. Ukshe, "Impedance of a silver electrode and the conductivity of a solid electrolyte of the nasicon type," *Soviet Electrochemistry*, vol. 22, no. 10, pp. 1240–1244, 1986.
- [5] J. Delhommelle, P. T. Cummings, and J. Petracic, "Conductivity of molten sodium chloride in an arbitrarily weak dc electric field," *The Journal of Chemical Physics*, vol. 123, no. 11, Article ID 114505, 2005.
- [6] G. H. Zimmerman, P. W. Scott, and W. Greynolds, "A new flow instrument for conductance measurements at elevated temperatures and pressures: Measurements on NaCl(aq) to 458 K and 1.4 MPa," *Journal of Solution Chemistry*, vol. 36, no. 6, pp. 767–786, 2007.
- [7] M. F. Butman, A. A. Smirnov, L. S. Kudin, and Z. A. Munir, "Mass-spectrometric study of the kinetics of ionic and molecular sublimation of sodium chloride single crystals," *Journal of Materials Synthesis and Processing*, vol. 7, no. 6, pp. 379–385, 2009.
- [8] M. L. V. Ramires, C. A. N. Decastro, J. Fareira, and W. A. Wakeham, "Thermal conductivity of aqueous sodium chloride solutions," *Journal of Chemical Engineering Data*, vol. 39, no. 1, pp. 186–190, 1994.
- [9] S. K. S. Basha, G. S. Sundari, K. V. Kumar, and M. C. Rao, "Preparation and dielectric properties of PVP-based polymer electrolyte films for solid-state battery application," *Polymer Bulletin*, pp. 1–21, 2017.
- [10] S. Rajendran, M. Sivakumar, and R. Subadevi, "Li-ion conduction of plasticized PVA solid polymer electrolytes complexed with various lithium salts," *Solid State Ionics*, vol. 167, no. 3-4, pp. 335–339, 2004.
- [11] H. Tsutsumi and A. Suzuki, "Cross-linked poly(oxetane) matrix for polymer electrolyte containing lithium ions," *Solid State Ionics*, vol. 262, pp. 761–764, 2014.
- [12] M. Wetjen, G.-T. Kim, M. Joost, M. Winter, and S. Passerini, "Temperature dependence of electrochemical properties of cross-linked poly(ethylene oxide)-lithium bis(trifluoromethanesulfonyl)imide-N-butyl-N-methylpyrrolidinium bis(trifluoromethanesulfonyl)imide solid polymer electrolytes for lithium batteries," *Electrochimica Acta*, vol. 87, pp. 779–787, 2013.
- [13] H.-Y. Wu, Y.-H. Chen, D. Saikia et al., "Synthesis, structure and electrochemical characterization, and dynamic properties of double core branched organic-inorganic hybrid electrolyte membranes," *Journal of Membrane Science*, vol. 447, pp. 274–286, 2013.
- [14] T. Zheng, Q. Zhou, Q. Li, L. Zhang, H. Li, and Y. Lin, "A new branched copolyether-based polymer electrolyte for lithium batteries," *Solid State Ionics*, vol. 259, pp. 9–13, 2014.
- [15] I. Barandiaran, A. Cappelletti, M. Strumia, A. Eceiza, and G. Kortaberria, "Generation of nanocomposites based on (PMMA-b-PCL)-grafted Fe₂O₃ nanoparticles and PS-b-PCL block copolymer," *European Polymer Journal*, vol. 58, pp. 226–232, 2014.
- [16] A. Sannigrahi, S. Takamuku, and P. Jannasch, "Block copolymers combining semi-fluorinated poly(arylene ether) and sulfonated poly(arylene ether sulfone) segments for proton exchange membranes," *International Journal of Hydrogen Energy*, vol. 39, no. 28, pp. 15718–15727, 2014.
- [17] N. Rakkapao, V. Vao-Soongnorn, Y. Masubuchi, and H. Watanabe, "Miscibility of chitosan/poly(ethylene oxide) blends and

- effect of doping alkali and alkali earth metal ions on chitosan/PEO interaction," *Polymer Journal*, vol. 52, no. 12, pp. 2618–2627, 2011.
- [18] S. Wang and K. Min, "Solid polymer electrolytes of blends of polyurethane and polyether modified polysiloxane and their ionic conductivity," *Polymer Journal*, vol. 51, no. 12, pp. 2621–2628, 2010.
- [19] Q. Cheng, Z. Cui, J. Li, S. Qin, F. Yan, and J. Li, "Preparation and performance of polymer electrolyte based on poly(vinylidene fluoride)/polysulfone blend membrane via thermally induced phase separation process for lithium ion battery," *Journal of Power Sources*, vol. 266, pp. 401–413, 2014.
- [20] J. Qiao, J. Fu, R. Lin, J. Ma, and J. Liu, "Alkaline solid polymer electrolyte membranes based on structurally modified PVA/PVP with improved alkali stability," *Polymer Journal*, vol. 51, no. 21, pp. 4850–4859, 2010.
- [21] T. J. Benedict, S. Banumathi, A. Veluchamy, R. Gangadharan, A. Z. Ahamad, and S. Rajendran, "Characterization of plasticized solid polymer electrolyte by XRD and AC impedance methods," *Journal of Power Sources*, vol. 75, no. 1, pp. 171–174, 1998.
- [22] J. Y. Cherng, M. Z. A. Munshi, B. B. Owens, and W. H. Smyrl, "Applications of multivalent ionic conductors to polymeric electrolyte batteries," *Solid State Ionics*, vol. 28–30, no. 1, pp. 857–861, 1988.
- [23] A. A. De Queiroz, D. A. Soares, P. Trzesniak, and G. A. Abraham, "Resistive-type humidity sensors based on PVP-Co and PVP-I2 complexes," *Journal of Polymer Science Part B: Polymer Physics*, vol. 39, no. 4, pp. 459–469, 2001.
- [24] R. M. Hodge, G. H. Edward, and G. P. Simon, "Water absorption and states of water in semicrystalline poly(vinyl alcohol) films," *Polymer Journal*, vol. 37, no. 8, pp. 1371–1376, 1996.
- [25] H. Feng, Z. Feng, and L. Shen, "A high resolution solid-state n.m.r. and d.s.c. study of miscibility and crystallization behaviour of poly(vinyl alcohol) poly(N-vinyl-2-pyrrolidone) blends," *Polymer Journal*, vol. 34, no. 12, pp. 2516–2519, 1993.
- [26] C. S. Ramya, S. Selvasekarapandian, and T. Savitha, "Proton-conducting membranes: Poly (N-vinyl pyrrolidone) complexes with various ammonium salts," *Journal of Solid State Electrochemistry*, vol. 12, no. 7–8, pp. 807–814, 2008.
- [27] M. Hema, S. Selvasekarapandian, G. Hirankumar, A. Sakunthala, D. Arunkumar, and H. Nithya, "Laser Raman and ac impedance spectroscopic studies of PVA: NH₄NO₃ polymer electrolyte," *Spectrochimica Acta Part A: Molecular and Biomolecular Spectroscopy*, vol. 75, no. 1, pp. 474–478, 2010.
- [28] D. Martin-Vosshage and B. V. R. Chowdari, "Characterization of poly(ethylene oxide) with cobaltbromide," *Solid State Ionics*, vol. 62, no. 3–4, pp. 205–216, 1993.
- [29] S. N. Cassu and M. I. Felisberti, "Poly(vinyl alcohol) and poly(vinyl pyrrolidone) blends: Miscibility, microheterogeneity and free volume change," *Polymer Journal*, vol. 38, no. 15, pp. 3907–3911, 1997.
- [30] M. Hema, S. Selvasekarapandian, H. Nithya, A. Sakunthala, and D. Arunkumar, "Structural and ionic conductivity studies on proton conducting polymer electrolyte based on polyvinyl alcohol," *Ionics*, vol. 15, no. 4, pp. 487–491, 2012.
- [31] S. K. S. Basha, G. S. Sundari, K. V. Kumar, and M. C. Rao, "Structural and dielectric properties of PVP based composite polymer electrolyte thin films," *Journal of Inorganic and Organometallic Polymers and Materials*, vol. 27, no. 2, pp. 455–466, 2017.
- [32] D. F. Varnell and M. M. Coleman, "FT i.r. studies of polymer blends: V. Further observations on polyester-poly(vinyl chloride) blends," *Polymer Journal*, vol. 22, no. 10, pp. 1324–1328, 1981.
- [33] M. M. Coleman and J. Zarian, "Fourier-transform infrared studies of polymer blends. II. Poly(ϵ -caprolactone)-poly(vinyl chloride) system," *Journal of Polymer Science Part B: Polymer Physics*, vol. 17, no. 5, pp. 837–850, 1979.
- [34] A. Garton, M. Aubin, and R. E. Prud'Homme, "FTIR of poly-caprolactone/poly(vinylidene chloride-co-acrylonitrile) miscible blends," *Journal of Polymer Science: Polymer Letters Edition*, vol. 21, no. 1, pp. 45–47, 1983.
- [35] D. F. Varnell, J. P. Runt, and M. M. Coleman, "FT i.r. and thermal analysis studies of blends of poly(ϵ -caprolactone) with homo- and copolymers of poly(vinylidene chloride)," *Polymer Journal*, vol. 24, no. 1, pp. 37–42, 1983.
- [36] E. M. Woo, J. W. Barlow, and D. R. Paul, "Phase behavior of blends of aliphatic polyesters with a vinylidene chloride/vinyl chloride copolymer," *Journal of Applied Polymer Science*, vol. 32, no. 3, pp. 3889–3897, 1986.
- [37] T. Nishi, T. T. Wang, and T. K. Kwei, "Thermally induced phase separation behavior of compatible polymer mixtures," *Macromolecules*, vol. 8, no. 2, pp. 227–234, 1975.
- [38] S. Chandra, S. A. Hashmi, and G. Prasad, "Studies on ammonium perchlorate doped polyethylene oxide polymer electrolyte," *Solid State Ionics*, vol. 40–41, no. 2, pp. 651–654, 1990.
- [39] M. Kumar and S. S. Sekhon, "Ionic conductance behaviour of plasticized polymer electrolytes containing different plasticizers," *Ionics*, vol. 8, no. 3–4, pp. 223–233, 2002.
- [40] W. Dieterich and P. Maass, "Non-debye relaxations in disordered ionic solids," *Chemical Physics*, vol. 284, no. 1–2, pp. 439–467, 2005.
- [41] R. C. Agrawal, S. A. Hashmi, and G. P. Pandey, "Electrochemical cell performance studies on all-solid-state battery using nanocomposite polymer electrolyte membrane," *Ionics*, vol. 13, no. 5, pp. 295–298, 2007.
- [42] R. D. Armstrong, T. Dickinson, and P. M. Willis, "The A.C. impedance of powdered and sintered solid ionic conductors," *Journal of Electroanalytical Chemistry*, vol. 53, no. 3, pp. 389–405, 1974.
- [43] W. Dieterich and P. Maass, "Non-Debye relaxations in disordered ionic solids," *Chemical Physics*, vol. 284, no. 1–2, pp. 439–467, 2002.
- [44] G. P. Pandey and S. A. Hashmi, "Performance of solid-state supercapacitors with ionic liquid 1-ethyl-3-methylimidazolium tris(pentafluoroethyl) trifluorophosphate based gel polymer electrolyte and modified MWCNT electrodes," *Electrochimica Acta*, vol. 105, pp. 333–341, 2013.
- [45] S. K. Basha and M. C. Rao, "Spectroscopic and electrochemical properties of PVP based polymer electrolyte films," *Polymer Bulletin*, 2017.
- [46] C. V. Subba Reddy, A. K. Sharma, and V. V. R. Narasimha Rao, "Conductivity and discharge characteristics of polyblend (PVP + PVA + KIO₃) electrolyte," *Journal of Power Sources*, vol. 114, no. 2, pp. 338–345, 2003.